



The Sources of Organic Carbon in the Deepest Ocean: Implication From Bacterial Membrane Lipids in the Mariana Trench Zone

Jiwei Li^{1,2†}, Zhiyan Chen^{1,3,4†}, Xinxin Li^{4,5}, Shun Chen¹, Hengchao Xu¹, Kaiwen Ta¹, Shamik Dasgupta¹, Shijie Bai¹, Mengran Du¹, Shuangquan Liu¹ and Xiaotong Peng^{1*}

¹ Institute of Deep-Sea Science and Engineering, Chinese Academy of Sciences, Beijing, China, ² Southern Marine Science and Engineering Guangdong Laboratory (Zhuhai), Sun Yat-sen University, Zhuhai, China, ³ School of Environment, Harbin Institute of Technology, Harbin, China, ⁴ Shenzhen Key Laboratory of Marine Archaea Geo-Omics, Department of Ocean Science and Engineering, Southern University of Science and Technology, Shenzhen, China, ⁵ Southern Marine Science and Engineering Guangdong Laboratory (Guangzhou), Guangzhou, China

OPEN ACCESS

Edited by:

Jiangong Wei,
Guangzhou Marine Geological Survey,
China

Reviewed by:

Wei Xie,
Sun Yat-sen University, Zhuhai
Campus, China
Hongxiang Guan,
Guangzhou Institute of Energy
Conversion (CAS), China

*Correspondence:

Xiaotong Peng
xtpeng1973@163.com

† These authors have contributed
equally to this work

Specialty section:

This article was submitted to
Geochemistry,
a section of the journal
Frontiers in Earth Science

Received: 15 January 2021

Accepted: 23 March 2021

Published: 13 April 2021

Citation:

Li J, Chen Z, Li X, Chen S, Xu H,
Ta K, Dasgupta S, Bai S, Du M, Liu S
and Peng X (2021) The Sources
of Organic Carbon in the Deepest
Ocean: Implication From Bacterial
Membrane Lipids in the Mariana
Trench Zone.
Front. Earth Sci. 9:653742.
doi: 10.3389/feart.2021.653742

Hadal trenches have higher microbial carbon turnover rates as compared to adjacent abyssal plains. However, the source of organic carbon in the trench remains enigmatic. In this study, we show that a fraction of organic carbon is possibly derived *in situ* and correlated with chemoautotrophic communities supported by the fluid discharge of water-rock interaction in the trench wall, based on analysis of glycerol dialkyl glycerol tetraether (GDGT) membrane lipids, including archaeal isoprenoid GDGTs (IsoGDGTs) and bacterial branched GDGTs (BrGDGTs), in sediments and rocks of the Mariana and Yap Trenches, northwest Pacific Ocean. These trench sediments contained relative higher BrGDGTs ratios, which was a rare observation in the open ocean. The BrGDGT-to-IsoGDGT ratios ranged in 0.02–0.88 (mean = 0.10 ± 0.11) in sediments and 0.09–0.38 (mean = 0.17 ± 0.13) in altered rocks. The calculated values of branched and isoprenoid tetraether (BIT) index ranged from 0.02–0.73 (mean = 0.18 ± 0.11) in sediments and from 0.16–0.9 in altered rocks (mean = 0.37 ± 0.27). Moreover, these GDGTs exhibited similar characteristics to those of altered basalt rocks, indicating inputs of organic carbon from the trench subsurface environment. Thus, in addition to organic-rich material settling, we propose chemoautotrophic activity in oceanic crust could be an additional source of organic carbon in the deepest part of the ocean, with an important role in deep-sea carbon cycles.

Keywords: hadal trenches, organic carbon, water-rock interaction, membrane lipids, deep-sea carbon cycles, chemoautotrophic activity

INTRODUCTION

Hadal trenches, which are located on the axis of subduction zones, are covered by water depths ranging from 6,500 m to 11,000 m and represent some of the most remote and least-explored regions on Earth (Jamieson et al., 2010; Jamieson et al., 2017, 2018). It has recently been revealed that there is a significantly higher microbial carbon turnover rate in hadal sediment than that in adjacent abyssal plain (Glud et al., 2013; Luo et al., 2018). This environment is also known to

sustain a diverse array of metazoan organisms (Jamieson et al., 2010) and heterotrophic microbial populations (Nunoura et al., 2015). It has been speculated that the supply of nutritious food at such great depths largely relied on the flux of fresh organic-rich particulate matter (Glud et al., 2013; Nunoura et al., 2015) and input of the decaying biota and carcasses from the upper ocean (Oguri et al., 2013). Moreover, low temperature water-rock interaction between bedrock and seawater, such as serpentinization and basalt rock alteration, is a common phenomenon at the bottom of trenches (Fryer et al., 1999; Stern et al., 2006; Du et al., 2019) and chemosynthetic microbial communities utilizing crustal fluid are also known to occur in trenches (Fujikura et al., 1999; Hand et al., 2012; Ohara et al., 2012). For example, the existence of fluid discharge features, including fluid discharge points and associated pockmarks, as well as chemosynthetic microorganisms, in the outer rise region was directly observed by submersible investigations in the southern Mariana trench (Du et al., 2019). Around these fluid discharge features, iddingsite-rich muds with high hydrogen and methane concentration were close association with augite, indicating the occurrence of iddingsitisation in these altered basalts (Du et al., 2019). However, the potential contribution of carbon fixation by these chemosynthetic microbial communities, which related to water-rock interaction, in the trench bottom remains enigmatic.

The membrane lipid GDGTs of prokaryotes, including IsoGDGTs and BrGDGTs (for structures see **Supplementary Figure 1**), in marine sediments are important biomarkers for tracing organic matter sources (Hopmans et al., 2004; Schouten et al., 2013; Weijers et al., 2014). BrGDGTs have been predominantly found in terrestrial settings such as soils and peat deposits. Although BrGDGTs may also be *in situ* formed in normal marine environments, the abundance of marine BrGDGTs differs from that of terrestrial soil by orders of magnitude (Peterse et al., 2009; Schouten et al., 2013; Weijers et al., 2014). The BIT index was proposed based on BrGDGTs and Crenarchaeol (representative of marine IsoGDGTs) contents (see **Supplementary Equations**) (Hopmans et al., 2004). In terrestrial soils, the BIT value is approximately 0.90 ± 0.14 , whereas that of open marine sediments is 0.04 ± 0.03 (Schouten et al., 2013). Therefore, this index is previously used to characterize the contribution of terrestrial soil inputs in marine environments (Schouten et al., 2013). However, several previous studies have found that relatively high BrGDGT content also presented in some chemoautotrophic systems, such as cold seep (Zhang et al., 2020), hydrothermal fields (Hu et al., 2012; Lincoln et al., 2013; Pan et al., 2016), and serpentinite-hosted ecosystems (Newman et al., 2020). These findings indicated that the high relative abundance of BrGDGT in the sedimentary environment of Open Ocean may be an indicator of the chemoautotrophic ecosystem.

To elucidate the source of organic matter at the bottom of trenches, we examined the GDGT lipid profiles of the sediments and rock samples retrieved from the southern Mariana Trench and northern Yap Trench, northwest Pacific Ocean. Our results demonstrated relatively high BrGDGT ratios within trench sediments, with similar composition to those of altered basaltic rocks rather than of sediments in open oceans, suggesting

chemoautotrophic carbon fixation in the subduction zone could be an effective source of organic carbon in the deepest parts of the ocean.

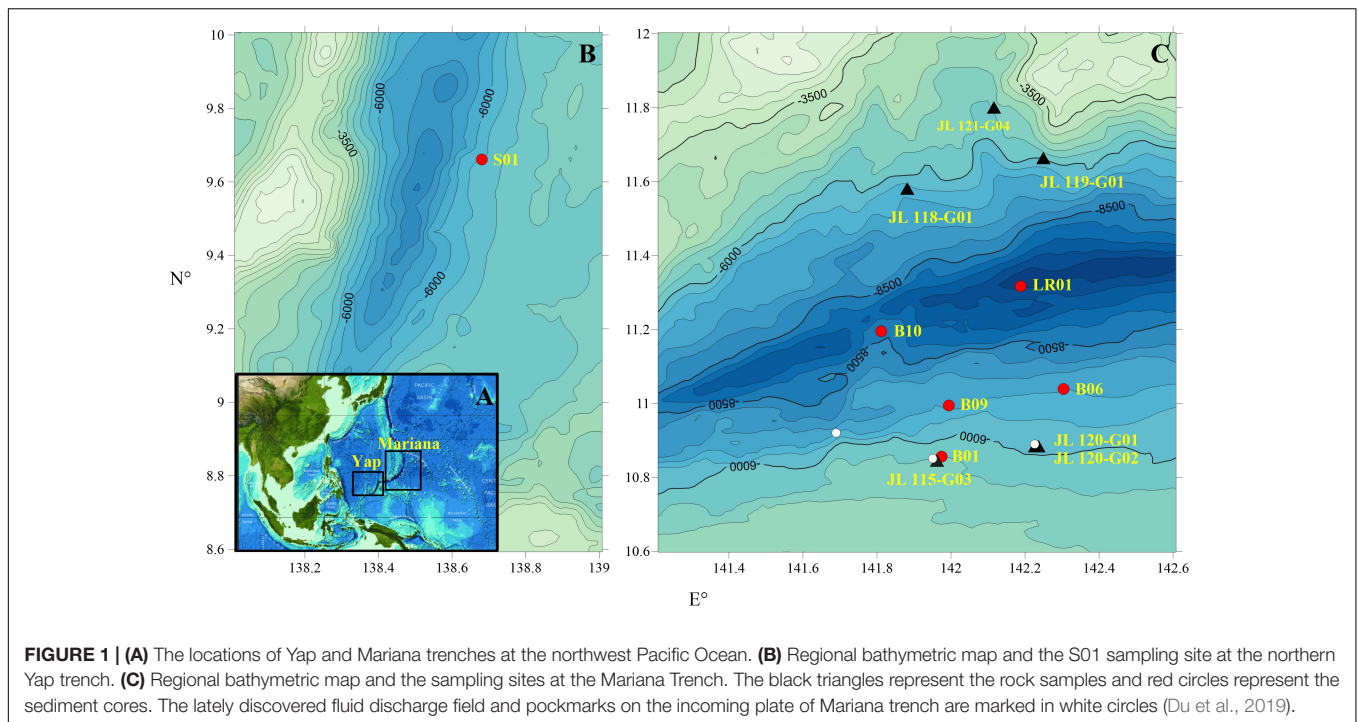
MATERIALS AND METHODS

Sample Collection

Sediment and rock samples were collected from the Yap and Mariana Trenches during cruises that were conducted in 2016 and 2017 (**Figure 1** and **Supplementary Table 1**). The multiple sediment core sample, S01, was collected from the northern Yap Trench at a water depth of 5,058 m using a sediment multi-core sampler on the R/V XIANG-YANG-HONG-09, during cruise DY-37 conducted by the China Ocean Mineral Resource R&D Association in 2016.

Nine dives (Dive 114-112) were also performed at the “Challenger deep” of Mariana trench by the “Jiaolong” Human Occupied Vehicle during cruise DY-37. On the two sides of the trench walls, a large number of rock fragments were scattered on the seafloor which is covered with thin sediments (**Supplementary Figures 2A-C**). These rock samples have undergone varying degrees of alteration. During dive 114 and 115, a few fluid discharging points (1 m in height and 2–5 m diameter) and small pockmarks (3–6 m in diameter) were observed at the southern wall with water depths ranging from 5,448 m to 6,669 m (Du et al., 2019). During dive 121, high altered basement rocks were observed at the Northern trench wall (**Supplementary Figure 2D**). A total of six rock samples (7 subsamples) were used in this study (**Supplementary Figure 3**). They were collected from the two sides of the “Challenger Deep”. Three samples, including JL118-G01, JL119-G01, and JL121-G04, were collected from northern wall with water depth ranging from 5,552 m to 6,697 m; while the other three samples JL115-G03, JL120-G01, and JL120-G02, were collected from its southern wall with water depths from 5,544 m to 6,296 m.

Four sediment box cores (B01, B06, B09, and B10) were collected from the southern Marianna Trench with a water depth from 5,525 m to 8,638 m using the box sediment sampler onboard the R/V TAN-SUO-YI-HAO, during cruise TS01 conducted by the Chinese Academy of Sciences in 2016. After the sediment boxes were collected on deck, short sediment cores were obtained by inserting PVC plastic pipes into the sediments. LR01 was a 23 cm long sediment core, and was sampled at the deepest site of the “Challenger Deep” onboard the R/V TAN-SUO-YI-HAO, during cruise TS03 conducted by the Chinese Academy of Sciences in 2017. It was collected by using the “Tianya” deep-sea Lander system, designed by the Institute of Deep-sea Science and Engineering, Chinese Academy of Sciences, with the features of sediment sampling, capturing macroorganisms and recording HD videos below 11,000 m water depth (**Supplementary Figure 4**). The sediment sampler of “Tianya” Lander, a cuboid cavity made of aluminum alloy, was installed at the foot of the lander frame, and inserted into the sediments by the dive gravity to complete the sampling process. The cores in each recovery were immediately sectioned into slices of 2 cm in thickness onboard, using an aseptic scalpel.



The LR01 sample was stored at -80°C , whereas the remaining sediment and altered rock samples were stored at -20°C . To avoid pollution, we removed the surface of rock sample using sterile hammer, cleaned with ethanol (70% v) and milliQ water after returning to the laboratory, and extracted the lipids from the interior part.

Lipids Analysis

In the laboratory, the selected sediments and rocks were ground into powders using an agate pestle and mortar after freeze-drying. An aliquot of each sample (5–10 g) was extracted ($\times 5$) ultrasonically with a mixture of dichloromethane and methanol (9:1, V/V) to obtain the total lipid extract. After condensation via a rotary evaporator, the extracted total lipids were further separated into alkanes and polar lipids using silica gel (60–100 mesh) flash column chromatography with *n*-hexane and methanol eluents, respectively. The polar fractions were then passed through 0.45- μm PTFE syringe filters and dried under a stream of nitrogen gas.

The *n*-alkanes and GDGTs were measured at the State Key Laboratory of Biogeology and Environmental Geology, China University of Geosciences (Wuhan), China. The aliphatic fraction containing *n*-alkanes was analyzed in an Agilent 6890 gas chromatography and 5,973 mass spectrometer (GC-MS), equipped with a silica capillary column (DB-5MS; 60 m \times 0.25 mm \times 0.25 μm). The GC oven temperature program for *n*-alkanes ramped from 50°C to 120°C at $8^{\circ}\text{C}/\text{min}$, and then from 120°C to 300°C at $5^{\circ}\text{C}/\text{min}$, held at 300°C for 20 min with helium as the carrier gas. The ionization energy was 70 eV and the temperature of interface between GC and MS was set as 280°C .

With respect to GDGTs analysis, the dried polar fraction was redissolved in *n*-hexane/isopropanol (99:1, v/v) for further analysis. Synthesized C_{46} GDGT was added as an internal standard in each redissolved sample. The GDGTs were analyzed using an Agilent 1200 series liquid chromatography tandem mass spectrometer, with ChemStation management software. Following injection by an autosampler, the GDGT compounds were separated using an Alltech Prevail Cyano column (150 mm \times 2.1 mm, 3 μm). Archaeal IsoGDGTs and bacterial BrGDGTs were then analyzed using single ion monitoring at m/z 1302, 1300, 1298, 1296, 1292, 1050, 1048, 1046, 1036, 1034, 1032, 1022, 1020, and 1018. A few GDGT isomers, including 5- and 6- methyl GDGTs could not be separated by using the single ion monitoring method of this study.

TOC, TN, and Carbon Stable Isotope Analysis

The total organic carbon (TOC), total nitrogen (TN), and carbon isotopic ($\delta^{13}\text{C}$) compositions of the sediments were measured at the State Key Laboratory of Biogeology and Environmental Geology, China University of Geosciences (Wuhan), China. The freeze-dried sediment samples were rapidly homogenized by grinding and weighed aliquots of the sample were acidified by adding 2 mL of 1 M HCl to every 100 mg of sample. The acidified samples were dried at $>60^{\circ}\text{C}$ under a stream of filtered air, then mixed with 1 mL of Milli-Q water and freeze-dried again. The samples were weighed again to account for the change in weight during the acid treatment. Aliquots of approximately 20 mg were added into 5 \times 8 mm tin capsules for the measurement of TOC, TN, and carbon isotopes ($\delta^{13}\text{C}$) using a continuous-flow isotope-ratio mass spectrometer (Delta V Advantage, Thermo

Scientific, Germany) coupled to an elemental analyzer (Flash EA 1112 Thermo Scientific, Italy) in the laboratory. The $\delta^{13}\text{C}$ results are expressed relative to Vienna PeeDee Belemnite. Replicates of an acetanilide standard (Thermo Scientific) were analyzed along with samples, which indicated that the analytical errors were $<0.1\text{‰}$ for $\delta^{13}\text{C}$. The C/N ratios were determined as mol/mol ratios, which were transformed from the %TOC and %TN weight data that were obtained as a part of the stable isotope analyses.

X-Ray Diffraction Analysis

After freeze-drying, the selected sediment and rock samples were thoroughly ground using a mortar and pestle before passing through a 200-mesh sieve. X-ray diffraction analyses were performed on the powdered sub-samples. Sample mounts were step scanned from 2.5° to 65° 2θ with a step size of 0.02° and 50 s counting time. The samples were run on a D/max2550VB3 + /PC X-ray diffractometer at 20 kV and 30 mA with CuK-alpha radiation (1.54061 \AA) and a graphite monochromator. Phase analyses were performed on a PDF2 (2004) computer with Jada 5.0 software.

RESULTS

Bulk Organic Geochemical Parameters

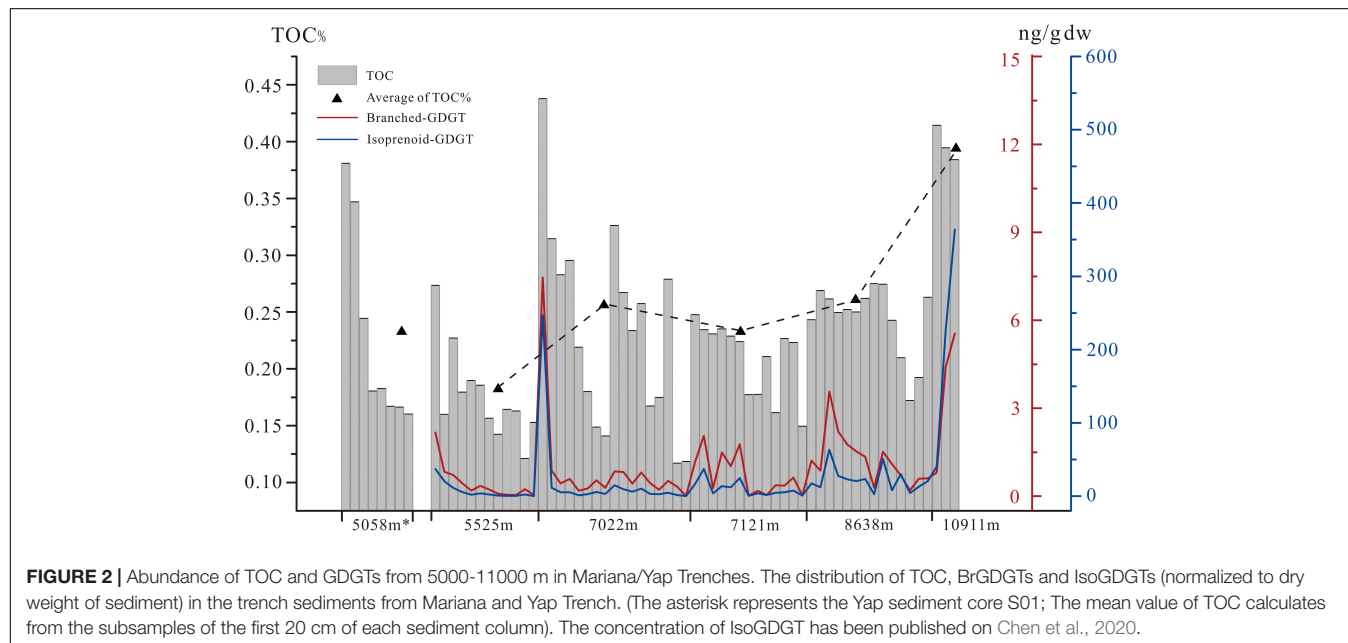
In this study, the abundance of TOC ranged from 0.12 to 0.42% in all sediment samples, with highest abundance at the core top sediment in B06 (1,0911 m) and lowest abundance at 33–34 cm of core B01 (5,525 m) (**Figure 2** and **Supplementary Table 2**). The $\delta^{13}\text{C}$ and C/N molar ratio of the bulk TOC of the sediment samples ranged between -21.72‰ and -16.70‰ (mean = $-19.02 \pm 1.05\text{‰}$, $n = 67$) and between 3.00 and 8.21 (mean = 4.96 ± 1.12 , $n = 67$), respectively, with no obvious trend

with the increasing water depth or core depth (**Supplementary Table 2** and **Figure 3**). As for reference site of 5,000 m water depth, mean TOC of S01 (5,058 m) in Yap Trench was a bit higher than that of B01 in Mariana Trench but still lower than other deeper sites. Therefore, the mean TOC of sediment cores of were generally increased with the increasing water depth in Mariana Trench. Regarding to each sediment core, TOC showed peak abundance at the surface (0–5 cm) of sediment core and fluctuatingly decreased with the sediment core depth (**Figure 2**).

GDGTs in Trench Sediments and Altered Rocks

The sum abundance of BrGDGT and IsoGDGT (Chen et al., 2020) in sediment was generally increased with increased water depth as TOC (**Figure 2**), varied from 0.02 to 7.48 ng/g dw and 0.16 to 363.85 ng/g dw, respectively. The distribution of the BrGDGTs was dominated by hexamethylated BrGDGTs (16–74%), followed by tetramethylated BrGDGTs (13–57%) and pentamethylated BrGDGTs (13–64%) (**Supplementary Table 2**). The domination of hexamethylated groups was coherent with another investigation of the sedimentary BrGDGTs in the bottom of Mariana trench (Xiao et al., 2019). The BrGDGT-to-IsoGDGT (Br/Iso) ratios ranged in 0.02–0.88 (mean = 0.10, $n = 67$) and 0.09–0.38 (mean = 0.17, $n = 7$). The calculated BIT values ranged in 0.02–0.73 (mean = 0.18, $n = 67$) (**Supplementary Table 2**). Approximately 58% of the sediment samples had BIT values over 0.15.

BrGDGTs of altered rock samples had also been identified. The sum abundance of BrGDGTs in these altered rock samples ranged from 0.03 to 0.41 ng/g dw. Similar distribution of BrGDGT composition was found in altered rock as in sediments. Dominated hexamethylated BrGDGTs were ranged from 44 to 72%, tetramethylated and pentamethylated groups contributed



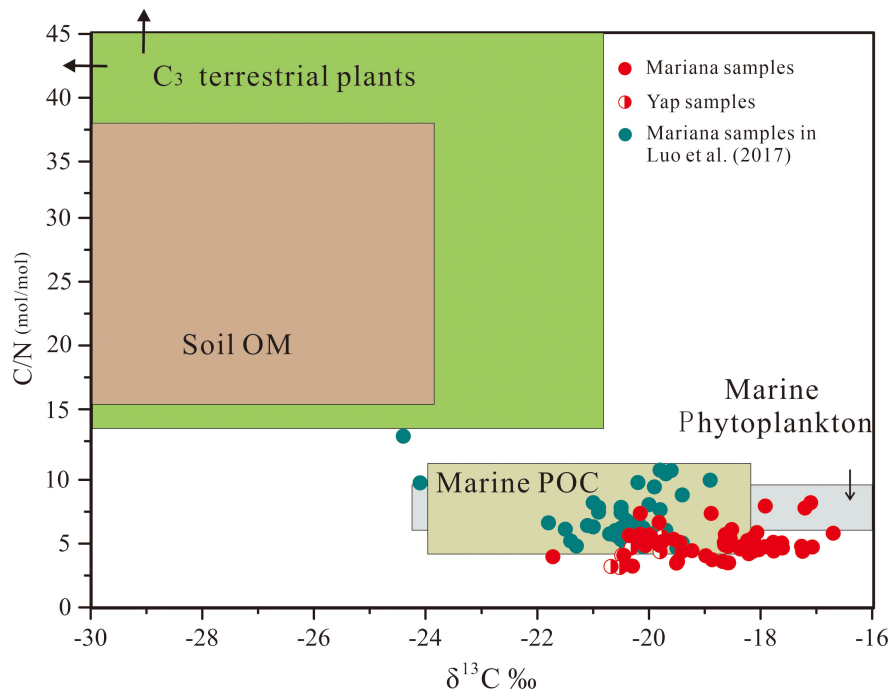


FIGURE 3 | Relationship between $\delta^{13}\text{C}$ of TOC and molar C/N ratios of organic matter. The domains of marine particle organic matter (Marine POC), marine phytoplankton, soil organic matter (Soil OM), and C₃ vascular plant are based on Goni et al., 2008; Khan et al., 2015 and references therein. The data of blue-green points in this figure are derived from Luo et al., 2017.

10–28% and 15–29%, respectively. Br/Iso ratio in altered rocks was ranged from 0.03 to 0.38 (mean = 0.17, $n = 7$). The calculated BIT values ranged in 0.16–0.90 (mean = 0.37, $n = 7$) (Supplementary Table 2).

n-Alkane and Related Index in Sediments

n-Alkanes in the range of C₁₆ – C₂₉ were mainly discovered in the trench sediments. The *n*-alkanes presented unimodal distribution pattern centered at C₂₁ – C₂₃ for S01 (5,058 m) and B01 (5,525 m), while centered at C₁₆ – C₁₈ for the sediment cores below 7,000 m without odd/even predominance (Figure 4). Inhomogeneous distribution of *n*-alkanes was found in both abundance and composition in trench sediments. The total *n*-alkanes concentrations ranged from 0.003 to 119.4 mg/g dw. The *n*-alkane of C₁₆ – C₁₈ were the major components that led to the increase in abundance of the total *n*-alkane below 7,000 m (Figure 4 and Supplementary Table 3). The average chain length (ACL) is the weight-averaged number of carbon atoms. The majority value ACL ranged from 17.0 to 22.7 (only one sample in B06 reached singularly high as 36.4). The carbon preference index (CPI) of C₁₅ – C₂₅ ranged from 0.37 to 3.82, with majority samples (65%) less than one (CPI < 1). Unresolved Complex Mixture (UCM) was obviously observed in most of the samples from trench slope (7,000–8,000 m) and several samples at 5,000 m sites in this study, accompanying with substantial branched alkanes and cycloalkanes indicated by Mass Spectrum (Supplementary Figure 5). UCM was presented for 73, 46, and

80% of the samples in B06 (7,022 m), B09 (7,121 m) and B10 (8,638 m), respectively.

Mineral Composition of the Sediments and Altered Rocks

We analyzed the mineral composition of selected sedimentary layers and all altered rocks samples. The X-ray diffraction results showed that quartz, feldspar, zeolite, montmorillonite, chlorite and halite were commonly detected in these sediment samples. While in these altered rocks, quartz, feldspar, chlorite, sepiolite, daubreelite, and talc were detected. Among them, it should be noted that zeolite presented in all of these altered rock samples (Supplementary Table 4).

DISCUSSION

Unusually High Proportions of BrGDGTs in Oceanic Trench Sediments and Altered Rocks

BrGDGTs have been reported in the trench sedimentary environments, such as the Mariana Trench (Ta et al., 2019; Xu et al., 2020), the Kermadec Trench (Xu et al., 2020), and Atacama Trench (Xu et al., 2020). One notable observation was that relative high abundance of BrGDGTs was examined at two sites with water depths shallower than 6,000 m in the Mariana trench (Ta et al., 2019). In consistent to result of Ta et al. (2019), our data further shows that approximately 58% of the sediment samples

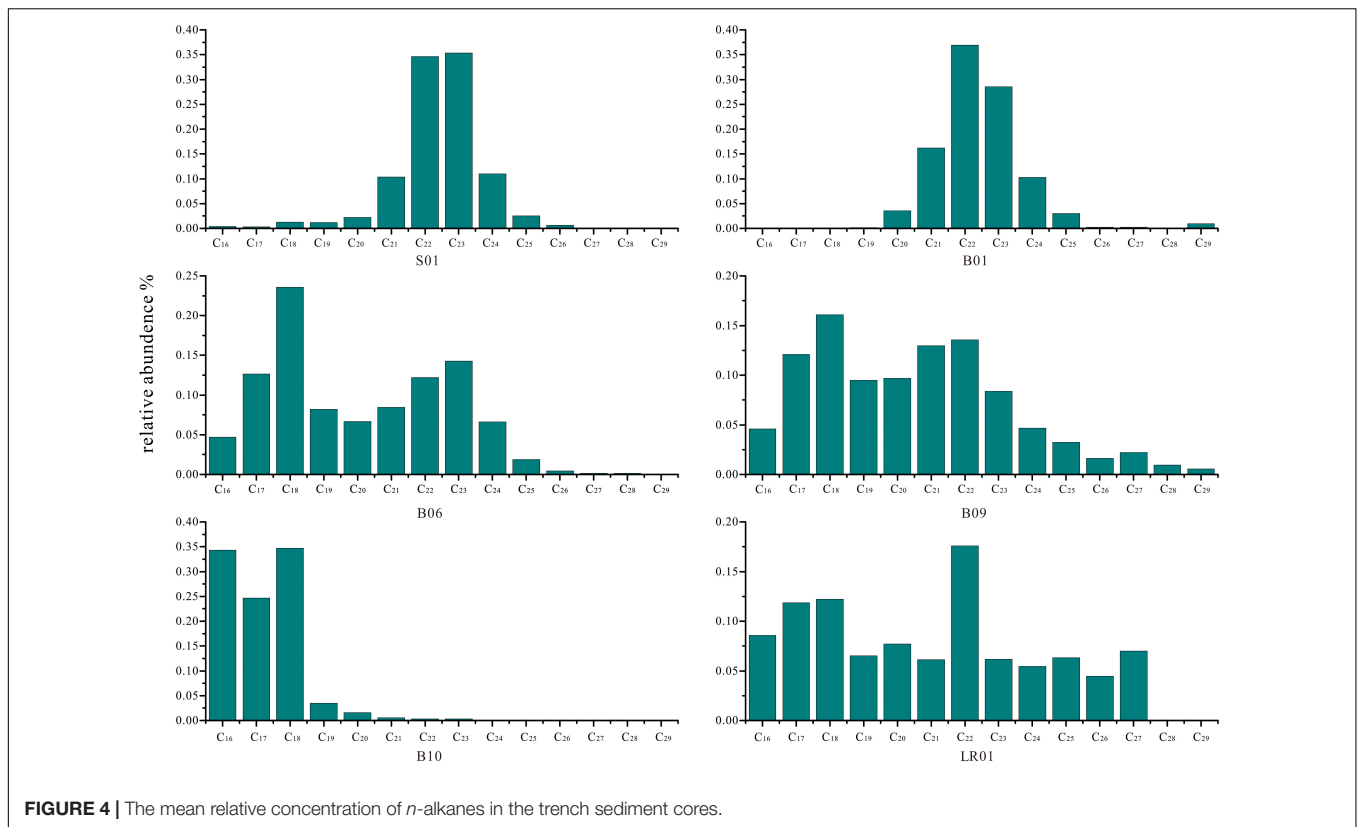


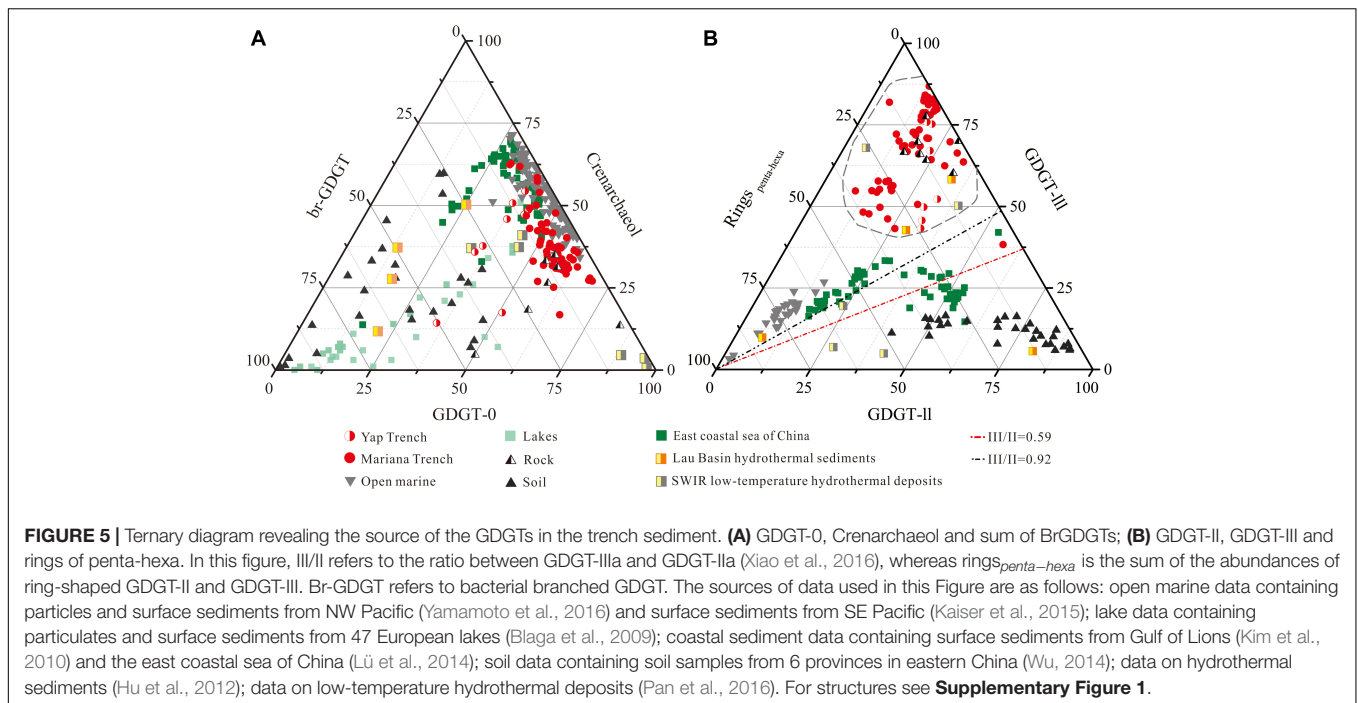
FIGURE 4 | The mean relative concentration of *n*-alkanes in the trench sediment cores.

had BIT values over 0.15. Although the BIT values of these trench sediments were lower than those observed in terrestrial soils, they were on average far greater than those previously reported for open marine sediments, and approached those of river mouth sediments (Weijers et al., 2014). However, the Mariana and Yap Trench are more than 2,000 km away from large landmasses, and marine production of IsoGDGTs rapidly dilutes the terrestrial BrGDGTs from river flows and dust inputs.

These BrGDGTs were possibly produced *in situ* in the ocean. The abundance ratio of hexamethylated to pentamethylated (IIIa/IIa) was inferred to be an indicator for BrGDGT source with higher values in deep sea sediments (2.6–5.1) than in soil (<0.59) (Xiao et al., 2016). BrGDGT was 3.87 ± 1.38 ($n = 67$) in the trench sediments (Supplementary Table 2), indicating little contribution of terrestrial soil inputs (Xiao et al., 2016). This conclusion was consistent with two recent studies, which reported that BrGDGTs in the Mariana trench were characterized by high cyclopentyl rings (Ta et al., 2019) and predominance of hexamethylated 6-methyl BrGDGT (Xiao et al., 2019). Furthermore, other organic geochemical indices also did not support its terrestrial origin. Typically, TOC/TN molar ratio of aquatic organic matter is restricted within values from ~ 4 to ~ 10 , and $\delta^{13}\text{C}$ from -34‰ to -12‰ (Lamb et al., 2006). Based on the bulk TOC/TN molar ratios (4.2–11) and $\delta^{13}\text{C}$ values of TOC (-21.8‰ to -18.9‰), Luo et al. (2017) suggested that the organic matter in the Mariana sediments was primarily marine origin. In this study, the TOC/TN molar ratio and $\delta^{13}\text{C}$ of the bulk organic matter of the sediment samples, which ranged

between 3.00 and 8.21 (mean = 4.96 ± 1.12 , $n = 67$) and between -21.72‰ and -16.70‰ (mean = $-19.02 \pm 1.05\text{‰}$, $n = 67$), respectively (Supplementary Table 2 and Figure 3), confirmed they were of marine sources (Lamb et al., 2006; Khan et al., 2015). This conclusion was also supported by the characteristics and distributions of *n*-alkanes in the trench sediments ($n < 27$, Figure 4 and Supplementary Table 3), with a dominance of short chain *n*-alkane and absence of odd-even preference (Nelson, 1978; Serrazanetti et al., 1995). Therefore, it seems likely that the measured BrGDGTs have formed by *in situ* production in the marine environment. Additionally, since the surface ocean and deep seawater column in this region have constant aerobic condition (Nunoura et al., 2015) and very low BrGDGT ratios (Schouten et al., 2013; Yamamoto et al., 2016), the relative abundance of BrGDGTs in trench sediments cannot be explained by funnelled inputs from the upper layers of the ocean. Therefore, the relative abundance of BrGDGTs in trench sediments might therefore be *in situ* production of the trench bottom (trench sediments or altered rocks).

Comparative analysis of trench sediment BrGDGT distributions with trench altered rocks and those from other sources suggests BrGDGTs in trench sediments were primarily derived from altered trench wall rocks. A ternary diagram of BrGDGT-Crenarchaeol-GDGT-0 abundance (Figure 5A) revealed significant differences between the GDGT characteristics of trench samples (both of sediments and altered rocks) and of terrestrial soil samples. Trench samples also showed higher levels of BrGDGTs and GDGT-0, on average,

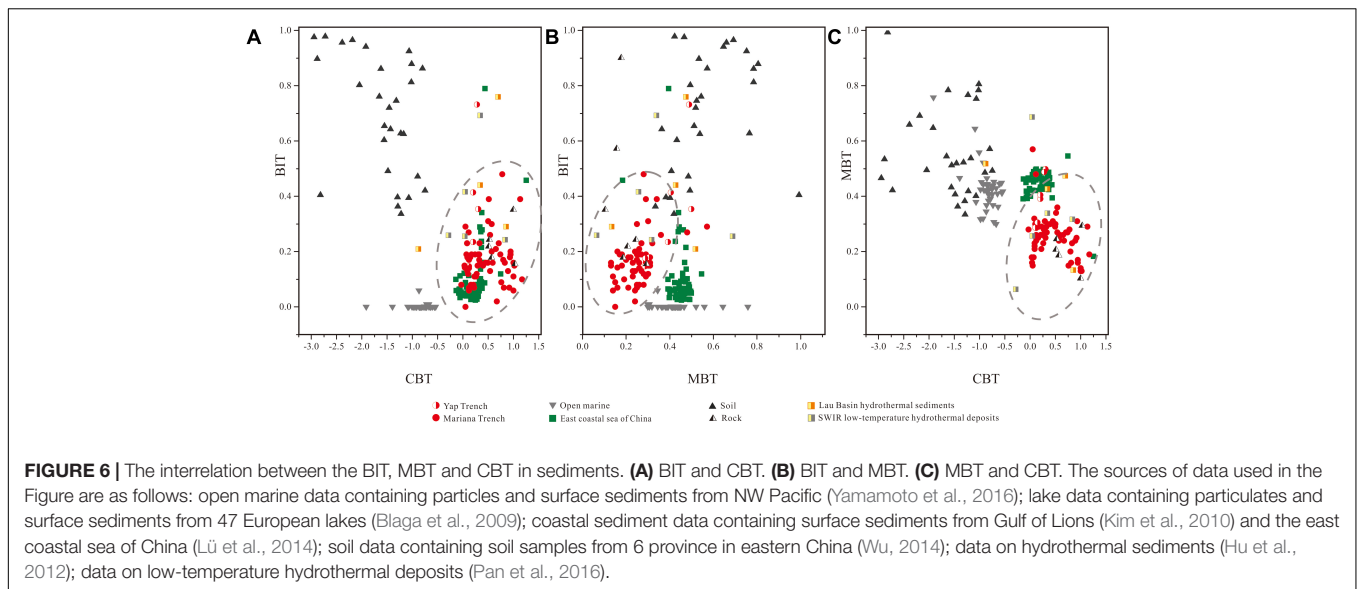


when compared to open marine sediments. When BrGDGTs alone were taken into consideration, a ternary diagram was drawn by plotting the composition of GDGT-II, GDGT-III, and $\text{Rings}_{\text{penta-hexa}}$ (the sum of GDGT-IIb, GDGT-IIc, GDGT-IIIb, and GDGT-IIIc) (**Figure 5B**). This result shows that the lipids of microbes in trench sediments differ significantly from those of waters nearby this region (Yamamoto et al., 2016) yet shared similar characteristics with lipids of microbes associated with altered rocks from this study and some previous reported hydrothermal sediment and deposits (Hu et al., 2012; Pan et al., 2016). This conclusion is further supported by comparative analysis of the interrelation between the BIT and two other parameters calculated from BrGDGTs, the methylation of branched tetraethers (MBT) and cyclization of branched tetraether (CBT) ratio (Weijers et al., 2007) [see the **Equation (2)** and **(3)**]. Again, the trench sediments cluster together with the altered trench wall rocks as well as some of the hydrothermal samples (**Figure 6**; Hu et al., 2012; Pan et al., 2016), characterized by higher CBT values and lower MBT values when compared to those of open ocean, soil and coastal sediments. Therefore, these results indicated that most part of BrGDGTs in the trench sediments might be sourced from the altered trench rocks.

Meanwhile, relatively high levels of BrGDGTs have also been reported in studies on chemoautotrophic systems, such as seafloor cold seep (Zhang et al., 2020), hydrothermal fields (Hu et al., 2012; Lincoln et al., 2013; Pan et al., 2016), and serpentinite-hosted ecosystems (Newman et al., 2020). For example, the BIT of hydrothermal sediments of the Lau Basin (Hu et al., 2012), and the low temperature hydrothermal deposits from the Southwest Indian Ridge (Pan et al., 2016) ranged in 0.1–0.76 and 0.24–0.69, respectively. Although they might not be directly sourced from these chemoautotrophic microorganisms

(Pan et al., 2016), they were likely derived from heterotrophic BrGDGT-producing bacteria which were fueled by the organic production from the chemoautotrophic communities (Pan et al., 2016). This inference was consistent with the recent findings by Weber et al. (2018), which reported that some BrGDGTs were indeed closely related to chemoautotrophic microorganisms under methanotrophic conditions. Having similar microbial composition is a sound explanation for the close BrGDGTs characteristics between trench sediments, altered rocks, and hydrothermal sediments and deposits. Additionally, widely distributed UCM in range of short carbon chain of hydrocarbon fractions in slope sediments may further indicated similar synthesis that found in petroleum contaminated or thermal reaction influenced sediments (Frysiner et al., 2003; McCollom et al., 2015), suggesting strongly biodegradation or weathering (Wenger and Isaksen, 2002; Hasinger et al., 2012). UCM in sediment of Mariana (4,000–7,000 m) was previously reported in Guan et al. (2019) which suggested UCM source from biodegraded oils with marine source and likely transported by normal faults and strike-slip faults on the seafloor (Tao et al., 2015; Guan et al., 2019).

In the hydrothermal microbial communities, one of the most conspicuous manifestations is the dominance of chemoautotrophic microorganisms. With regard to the marine trenches, chemoautotrophic communities are far from uncommon (Fujikura et al., 1999; Hand et al., 2012; Ohara et al., 2012). On one hand, the geological settings of the trench bottom can provide habitat niches (e.g., methanotrophic and ammonia oxidizing conditions) for chemolithoautotrophic life (Spang et al., 2010; Nunoura et al., 2015, 2018). The distribution of IsoGDGT in Mariana Trench revealed increasing presence of deep dwelling ammonia oxidizing archaeal group



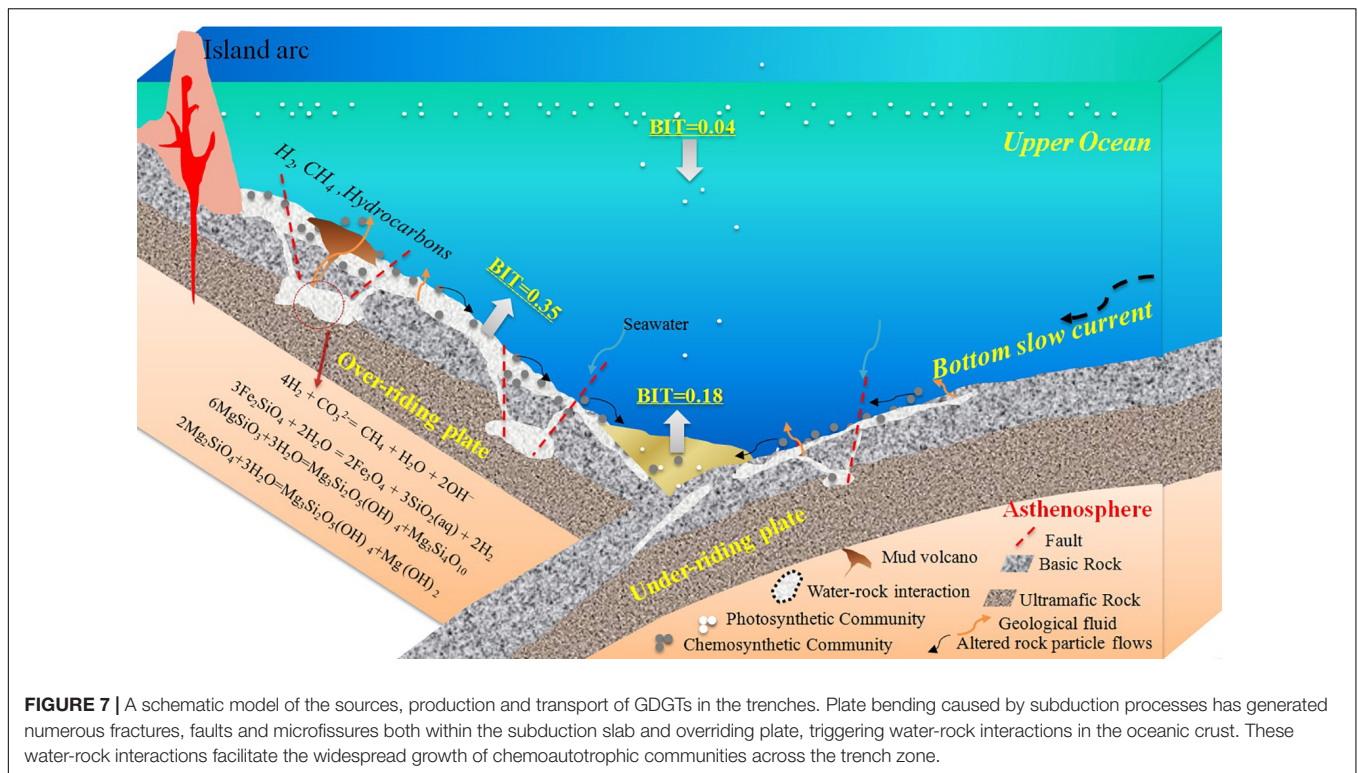
(*Thaumarchaeota*) in the sediments (Chen et al., 2020). On the other hand, chemolithoautotrophic group of CH_4 and H_2 utilizing in sediment may raise its attention based on conspicuous abundance of dissolved H_2 and H_2 -utilizing chemolithotrophs that were recently identified in the altered rocks and muds of the fluid discharge field at the incoming plate of the southern Mariana trench (Du et al., 2019). Meanwhile, the process of serpentinization, which can generate substantial amounts of crustal fluids for microbial CH_4 and H_2 utilization, has been reported to widely occur at the southern Mariana forearc (Ohara et al., 2012; Plümper et al., 2017). Moreover, Tarn et al. (2016) suggested that the microbial communities of Mariana Trench bottom water indeed characteristically display a degree of overlap with microbial communities from low-temperature diffuse flow hydrothermal vents and deep-subsurface locations. Specifically, taxa frequently encountered in vent datasets, such as *Gammaproteobacteria*, *Epsilonproteobacteria*, SAR324, *Thiovulgaceae*, and *SUP05*, were also detected in the trench sediments (Tarn et al., 2016). In addition, abundant of hydrocarbon-degrading bacteria and unknown sources of alkanes were also unexpectedly detected in the sediment of the Mariana trench (Li et al., 2019; Liu et al., 2019). This phenomenon may also be related to the activity of water-rock interaction in the trench bottom (Li et al., 2019). Overall, high similarity in GDGTs between the trench sediments and altered rocks together with these previous microbial and geochemical evidence might imply the wide distribution of chemoautotrophically-based microbial communities in the trench walls, supported by active geological fluid discharge from water-rock interaction.

The Schematic Model of Chemoautotrophic Organic Carbon Production in the Trench Zone

We proposed a schematic model to explore this relationship between water-rock interaction and chemoautotrophic

organic carbon in the trench zone (Figure 7). On one hand, fluid discharge and mud volcanoes induced by large-scale serpentinization were widely distributed along the forearc of the Mariana Trench (Fryer et al., 1999; Stern et al., 2006). The chemoautotrophic communities fed by these fluids have been reported in the literature. For example, the serpentinization-formed “Shinkai Seep Field” was discovered at the Southern Mariana Forearc (Ohara et al., 2012). Based on this discovery, they proposed that fluid discharge from serpentinization could be widespread in oceanic trenches. Moreover, Plümper et al. (2017) found organic matter encapsulated in rock clasts from an oceanic serpentinite mud volcano above the Izu–Bonin–Mariana subduction zone. Because of this result, they predicted that the serpentinization-fueled systems in the hydrated forearc mantle of Mariana subduction zone may represent one of Earth’s largest hidden microbial ecosystems. On the other hand, low-temperature alteration reactions between basaltic rocks and seawater also would be a pervasive phenomenon in the trench environments. This conclusion is supported by the common detection of zeolite in the trench sediments and altered rocks (Supplementary Table 4). Zeolite is possibly formed by the low-temperature hydrothermal alteration of basalt (Liou, 1979). This process can also fuel the chemoautotrophic communities, which constitute a trophic base of the basalt habitat in the oceanic crust (Cowen et al., 2003; Santelli et al., 2008). At present, chemoautotrophic carbon fixation associated with carbon and sulfur cycling in seafloor basalts has been proved by multiple lines of indirect evidence, such as depletions in $\delta^{34}\text{S}$ -pyrite (Rouxel et al., 2008) and DNA sequences (Cowen et al., 2003; Orcutt et al., 2011; Lever et al., 2013). Additionally, the occurrence of fluids discharge feature and H_2 -utilizing chemolithotrophs (Du et al., 2019) in the outer rise zone of the incoming plate at the southern Mariana trench further supported this conclusion.

In our schematic model, the plate bending caused by subduction processes has generated numerous faults, fractures and microfissures, both within the outer rise zone of the



subduction slab and the forearc of the overriding plate, which provides channels for the influx of water into the oceanic crust, thereby triggering water-rock interactions on a large scale. The geological fluids generated by these interactions are then released in the same channels from the oceanic crust. The fluids are rich in hydrogen, methane, hydrocarbons, and other reduced inorganic matter (e.g., Fe, Mn, and S), making them excellent substrates for chemoautotrophic microorganisms. These water-rock interactions facilitate the widespread growth of chemoautotrophic communities across the trench. As shown in **Supplementary Figure 6**, an increasing trend of BIT was observed in S01, B01 and B06, that corresponds to results in Ta et al. (2019), where an identical trend from surface to bottom was reported in a meter-long sediment core recovered from the Mariana Trench subduction zone (~5000 m). Higher BIT values in the core bottom at water depths of 5,000–7,000 m, underlain by subducted oceanic crust, suggested abnormal distribution of BrGDGT, compared to those recorded from open oceans with low BIT values. However, such distribution pattern was weak or even reversed at deeper water sites (see B09 and B10). Previously, low BIT values were reported in the sediment cores at the bottom of the Trench (~11,000 m) by Xiao et al. (2019), which is in line with our findings in core LR01. We speculate that with weakening tectonic distortion of the subducted plate at deeper water depths, increasing BIT values are rarely observed at surface and subsurface sediment (at least 40 cm in this study).

Finally, in the schematic model, the excess labile organic matter produced by these communities are transported laterally to the deeper parts of the trenches through gravity flows, leading to relatively higher microbial carbon turnover rate. No direct

evidence of synthesis of BrGDGTs by the chemoautotrophic group is evident yet. However, increasing trend of BIT values from surface to bottom core at subduction zones, and similar composition of BrGDGTs with altered rocks and minerals implies a strong connection between the ecology shaped by chemical fluids in deep sediments and microbial synthesizers of BrGDGT. Overall, we propose that chemoautotrophy driven by geological activity could be an effective supplement to the trench organic carbon pool in addition to photosynthetic products sourced from the upper ocean.

CONCLUSION

In this study, mineralogical compositions, bulk organic geochemical parameters and membrane lipids compositions were examined in sediments and rocks of the Mariana and Yap Trenches, northwest Pacific Ocean. The results shown that these trench sediments and altered rocks contained relative higher BrGDGTs contents, with the BrGDGT-to-IsoGDGT ratios ranged in 0.02–0.88 (mean = 0.10 ± 0.11) and 0.09–0.38 (mean = 0.17 ± 0.13), respectively. Meanwhile, the BIT index ranged in 0.02–0.73 (mean = 0.18 ± 0.11) in sediments and from 0.16–0.9 in altered rocks (mean = 0.37 ± 0.27), which are much higher than those of open ocean. Together with bulk TOC, TN and *n*-alkanes data, we suggested that these BrGDGTs were *in situ* production in the trench zone. Furthermore, these GDGTs exhibited similar characteristics to those of altered basalt rocks, indicating a fraction of organic carbon was possibly derived from chemoautotrophic communities supported by the fluid discharge

of water-rock interaction in the trench walls. This was further supported by the common detection of zeolite, indicative of water-rock alteration, in both altered rocks and trench sediments. Thus, we propose chemoautotrophic activity in oceanic crust could be an additional source of organic carbon in the trench sedimentary environments.

DATA AVAILABILITY STATEMENT

The datasets presented in this study can be found in online repositories. The names of the repository/repositories and accession number(s) can be found below: <https://doi.org/10.5281/zenodo.3551342>.

AUTHOR CONTRIBUTIONS

XP devised the project. JL provided the main conceptual ideas and wrote the manuscript. ZC worked out almost all of the experiments and performed the numerical calculations. XL and SD worked with the analysis of membrane lipid data. SC, HX, and KT helped with the sampling in voyages. SB, MD, and SL worked

in technical details and part of mineral data analysis. All authors contributed to the article and approved the submitted version.

FUNDING

This study was financially supported by the National Key Research and Development Project of China (No. 2017YFC0306604), the National Key Basic Research Program of China (No. 2015CB755905), the National Natural Science Foundation of China (Nos. 41576038 and 41876050), and the Youth Innovation Promotion Association CAS to JL, Shenzhen international collaborative research project (No. GJHZ20180928155004783), and Shenzhen Key Laboratory of Marine Archaea Geo-Omics, Southern University of Science and Technology (No. ZDSYS20180208184349083) to XL.

SUPPLEMENTARY MATERIAL

The Supplementary Material for this article can be found online at: <https://www.frontiersin.org/articles/10.3389/feart.2021.653742/full#supplementary-material>

REFERENCES

- Bлга, C. I., Reichart, G.-J., Heiri, O., and Sinninghe Damsté, J. S. (2009). Tetraether membrane lipid distributions in water-column particulate matter and sediments: a study of 47 European lakes along a north-south transect. *J. Paleolimnol.* 41, 523–540. doi: 10.1007/s10933-008-9242-2
- Chen, Z., Li, J., Li, X., Chen, S., Dasgupta, S., Bai, S., et al. (2020). Characteristics and implications of isoprenoid and hydroxy tetraether lipids in hadal sediments of Mariana and Yap Trenches. *Chem. Geol.* 551:119742. doi: 10.1016/j.chemgeo.2020.119742
- Cowen, J. P., Giovannoni, S. J., Kenig, F., Johnson, H. P., Butterfield, D., Rappé, M.S., et al. (2003). Fluids from Aging Ocean Crust That Support Microbial Life. *Science* 299, 120–123. doi: 10.1126/science.1075653
- Du, M., Peng, X., Seyfried, W. E. Jr., Ka, T., Guo, Z., Chen, S., et al. (2019). Fluid discharge linked to bending of the incoming plate at the Mariana subduction zone. *Geochem. Perspect. Lett.* 11, 1–5. doi: 10.7185/geochemlet.1916
- Fryer, P., Wheat, C. G., and Mottl, M. J. (1999). Mariana blueschist mud volcanism: implications for conditions within the subduction zone. *Geology* 27, 103–106. doi: 10.1130/0091-7613(1999)027<0103:MBMVIF>2.3.CO;2
- Frysinger, G. S., Gaines, R. B., Xu, L., and Reddy, C. M. (2003). Resolving the Unresolved Complex Mixture in Petroleum-Contaminated Sediments. *Environ. Sci. Technol.* 37, 1653–1662. doi: 10.1021/es020742n
- Fujikura, K., Kojima, S., Tamaki, K., Maki, Y., Hunt, J., and Okutani, T. (1999). The deepest chemosynthesis-based community yet discovered from the hadal zone, 7326 m deep, in the Japan Trench. *Mar. Ecol. Prog. Ser.* 190, 17–26. doi: 10.3354/meps190017
- Glud, R. N., Wenzhöfer, F., Middelboe, M., Oguri, K., Turnewitsch, R., Canfield, D. E., et al. (2013). High rates of microbial carbon turnover in sediments in the deepest oceanic trench on Earth. *Nat. Geosci.* 6, 284–288. doi: 10.1038/ngeo1773
- Goni, M. A., Monacci, N., Gisewhite, R., Crockett, J., Nittrouer, C., Ogston, A., et al. (2008). Terrigenous organic matter in sediments from the Fly River delta-clinofan system (Papua New Guinea). *J. Geophys. Res.* 113:F01S10. doi: 10.1029/2006JF000653
- Guan, H., Chen, L., Luo, M., Liu, L., Mao, S., Ge, H., et al. (2019). Composition and origin of lipid biomarkers in the surface sediments from the southern Challenger Deep, Mariana Trench. *Geosci. Front.* 10, 351–360. doi: 10.1016/j.gsf.2018.01.004
- Hand, K. P., Bartlett, D. H., Fryer, P., et al. (2012). *Analyses Of Outcrop And Sediment Grains Observed And Collected From The Sirena Deep And Middle Pond Of The Mariana Trench*. Washington, DC: AGU Fall Meeting.
- Hasinger, M., Scherr, K. E., Lundaa, T., Bräuer, L., Zach, C., and Loibner, A. P. (2012). Changes in iso- and n-alkane distribution during biodegradation of crude oil under nitrate and sulphate reducing conditions. *J. Biotechnol.* 157, 490–498. doi: 10.1016/j.jbiotec.2011.09.027
- Hopmans, E. C., Weijers, J. W. H., Schefuß, E., Herfort, L., Sinninghe Damsté, J. S., and Schouten, S. (2004). A novel proxy for terrestrial organic matter in sediments based on branched and isoprenoid tetraether lipids. *Earth Planet. Sci. Lett.* 224, 107–116. doi: 10.1016/j.epsl.2004.05.012
- Hu, J., Meyers, P. A., Chen, G., Peng, P., and Yang, Q. (2012). Archaeal and bacterial glycerol dialkyl glycerol tetraethers in sediments from the Eastern Lau Spreading Center, South Pacific Ocean. *Org. Geochem.* 43, 162–167. doi: 10.1016/j.orggeochem.2011.10.012
- Jamieson, A. J., Fang, J., and Cui, W. (2018). Exploring the Hadal Zone: recent Advances in Hadal Science and Technology. *Deep Sea Res. II Top. Stud. Oceanogr.* 155, 1–3. doi: 10.1016/j.dsr2.2018.11.007
- Jamieson, A. J., Fujii, T., Mayor, D. J., Solan, M., and Priede, I. G. (2010). Hadal trenches: the ecology of the deepest places on Earth. *Trends Ecol. Evol.* 25, 190–197. doi: 10.1016/j.tree.2009.09.009
- Jamieson, A. J., Malkocs, T., Piertney, S. B., Fujii, T., and Zhang, Z. (2017). Bioaccumulation of persistent organic pollutants in the deepest ocean fauna. *Nat. Ecol. Evol.* 1:51. doi: 10.1038/s41559-016-0051
- Kaiser, J., Schouten, S., Kilian, R., Arz, H. W., Lamy, F., and Sinninghe Damsté, J. S. (2015). Isoprenoid and branched GDGT-based proxies for surface sediments from marine, fjord and lake environments in Chile. *Org. Geochem.* 8, 117–127. doi: 10.1016/j.orggeochem.2015.10.007
- Khan, N. S., Vane, C. H., and Horton, B. P. (2015). “Stable carbon isotope and C/N geochemistry of coastal wetland sediments as a sea-level indicator,” in *Handbook of Sea-Level Research*, eds I. Shennan, A. J. Long, and B. P. Horton (Chichester, UK: John Wiley & Sons Ltd), 295–311. doi: 10.1002/9781118452547.ch20
- Kim, J.-H., Zarzycka, B., Buscail, R., Peterse, F., Bonnin, J., Ludwig, W., et al. (2010). Contribution of river-borne soil organic carbon to the Gulf of Lions (NW Mediterranean). *Limnol. Oceanogr.* 55, 507–518. doi: 10.4319/lo.2010.55.2.0507
- Lamb, A. L., Wilson, G. P., and Leng, M. J. (2006). A review of coastal palaeoclimate and relative sea-level reconstructions using $\delta^{13}\text{C}$ and C/N ratios in organic material. *Earth Sci. Rev.* 75, 29–57. doi: 10.1016/j.earscirev.2005.10.003

- Lever, M. A., Rouxel, O., Alt, J. C., Shimizu, N., Ono, S., Coggon, R. M., et al. (2013). Evidence for microbial carbon and sulfur cycling in deeply buried ridge flank basalt. *Science* 339, 1305–1308. doi: 10.1126/science.1229240
- Li, W.-L., Huang, J.-M., Zhang, P.-W., Cui, G.-J., Wei, Z.-F., Wu, Y.-Z., et al. (2019). Periodic and Spatial Spreading of Alkanes and *Alcanivorax* Bacteria in Deep Waters of the Mariana Trench. *Appl. Environ. Microbiol.* 85, e02089–18. doi: 10.1128/AEM.02089-18
- Lincoln, S. A., Bradley, A. S., Newman, S. A., and Summons, R. E. (2013). Archaeal and bacterial glycerol dialkyl glycerol tetraether lipids in chimneys of the Lost City Hydrothermal Field. *Org. Geochem.* 60, 45–53. doi: 10.1016/j.orggeochem.2013.04.010
- Liou, J. G. (1979). Zeolite facies metamorphism of basaltic rocks from the East Taiwan ophiolite. *Am. Mineral.* 64, 1–14.
- Liu, J., Zheng, Y., Lin, H., Wang, X., Li, M., Liu, Y., et al. (2019). Proliferation of hydrocarbon-degrading microbes at the bottom of the Mariana Trench. *Microbiome* 7:47. doi: 10.1186/s40168-019-0652-3
- Lü, X., Yang, H., Song, J., Versteegh, G. J. M., Li, X., Yuan, H., et al. (2014). Sources and distribution of isoprenoid glycerol dialkyl glycerol tetraethers (GDGTs) in sediments from the east coastal sea of China: application of GDGT-based paleothermometry to a shallow marginal sea. *Org. Geochem.* 75, 24–35. doi: 10.1016/j.orggeochem.2014.06.007
- Luo, M., Gieskes, J., Chen, L., Shi, X., and Chen, D. (2017). Provenances, distribution, and accumulation of organic matter in the southern Mariana Trench rim and slope: implication for carbon cycle and burial in hadal trenches. *Mar. Geol.* 386, 98–106. doi: 10.1016/j.margeo.2017.02.012
- Luo, M., Glud, R. N., Pan, B., Wenzhöfer, F., Xu, Y., Lin, G., et al. (2018). Benthic Carbon Mineralization in Hadal Trenches: insights From In Situ Determination of Benthic Oxygen Consumption. *Geophys. Res. Lett.* 45, 2752–2760. doi: 10.1002/2017GL076232
- McCollom, T. M., Seewald, J. S., and German, C. R. (2015). Investigation of extractable organic compounds in deep-sea hydrothermal vent fluids along the Mid-Atlantic Ridge. *Geochim. Cosmochim. Acta* 156, 122–144. doi: 10.1016/j.gca.2015.02.022
- Nelson, D. R. (1978). Long-Chain Methyl-Branched Hydrocarbons: occurrence, Biosynthesis, and Function. *Adv. Insect Physiol.* 13, 1–33. doi: 10.1016/S0065-2806(08)60263-5
- Newman, S. A., Lincoln, S. A., O'Reilly, S., Liu, X., Shock, E. L., Kelemen, P. B., et al. (2020). Lipid Biomarker Record of the Serpentinite-Hosted Ecosystem of the Samail Ophiolite, Oman and Implications for the Search for Biosignatures on Mars. *Astrobiology* 20, 830–845. doi: 10.1089/ast.2019.2066
- Nunoura, T., Nishizawa, M., Hirai, M., Shimamura, S., Harnvoravongchai, P., Koide, O., et al. (2018). Microbial Diversity in Sediments from the Bottom of the Challenger Deep, the Mariana Trench. *Microbes Environ.* 33, 186–194. doi: 10.1264/jisme.2.ME17194
- Nunoura, T., Takaki, Y., Hirai, M., Shimamura, S., Makabe, A., Koide, O., et al. (2015). Hadal biosphere: insight into the microbial ecosystem in the deepest ocean on Earth. *Proc. Natl. Acad. Sci. U. S. A.* 112, E1230–6. doi: 10.1073/pnas.1421816112
- Oguri, K., Kawamura, K., Sakaguchi, A., Toyofuku, T., Kasaya, T., Murayama, M., et al. (2013). Hadal disturbance in the Japan Trench induced by the 2011 Tohoku–Oki Earthquake. *Sci. Rep.* 3:1915. doi: 10.1038/srep01915
- Ohara, Y., Reagan, M. K., Fujikura, K., Watanabe, H., Michibayashi, K., Ishii, T., et al. (2012). A serpentinite-hosted ecosystem in the Southern Mariana Forearc. *Proc. Natl. Acad. Sci. U. S. A.* 109, 2831–2835. doi: 10.1073/pnas.1112005109
- Orcutt, B. N., Bach, W., Becker, K., Fisher, A. T., Hentscher, M., Toner, B. M., et al. (2011). Colonization of subsurface microbial observatories deployed in young ocean crust. *ISME J.* 5, 692–703. doi: 10.1038/ismej.2010.157
- Pan, A., Yang, Q., Zhou, H., Ji, F., Wang, H., and Pancost, R. D. (2016). A diagnostic GDGT signature for the impact of hydrothermal activity on surface deposits at the Southwest Indian Ridge. *Org. Geochem.* 99, 90–101. doi: 10.1016/j.orggeochem.2016.07.001
- Peterse, F., Kim, J.-H., Schouten, S., Kristensen, D. K., Koç, N., and Sinninghe Damsté, J. S. (2009). Constraints on the application of the MBT/CBT palaeothermometer at high latitude environments (Svalbard, Norway). *Org. Geochem.* 40, 692–699. doi: 10.1016/j.orggeochem.2009.03.004
- Plümper, O., King, H. E., Geisler, T., Liu, Y., Pabst, S., Savov, I. P., et al. (2017). Subduction zone forearc serpentinites as incubators for deep microbial life. *Proc. Natl. Acad. Sci. U. S. A.* 114, 4324–4329. doi: 10.1073/pnas.1612147114
- Rouxel, O., Ono, S., Alt, J., Rumble, D., and Ludden, J. (2008). Sulfur isotope evidence for microbial sulfate reduction in altered oceanic basalts at ODP Site 801. *Earth Planet. Sci. Lett.* 268, 110–123. doi: 10.1016/j.epsl.2008.01.010
- Santelli, C. M., Orcutt, B. N., Banning, E., Bach, W., Moyer, C. L., Sogin, M. L., et al. (2008). Abundance and diversity of microbial life in ocean crust. *Nature* 453, 653–657.
- Schouten, S., Hopmans, E. C., and Sinninghe Damsté, J. S. (2013). The organic geochemistry of glycerol dialkyl glycerol tetraether lipids: a review. *Org. Geochem.* 54, 19–61. doi: 10.1016/j.orggeochem.2012.09.006
- Serrazanetti, G. P., Pagnucco, C., Conte, L. S., and Cattani, O. (1995). Hydrocarbons, sterols and fatty acids in sea urchin (*Paracentrotus lividus*) of the adriatic sea. *Chemosphere* 30, 1453–1461. doi: 10.1016/0045-6535(95)00039-B
- Spang, A., Hatzenpichler, R., Brochier-Armanet, C., Rattei, T., Tischler, P., Spieck, E., et al. (2010). Distinct gene set in two different lineages of ammonia-oxidizing archaea supports the phylum Thaumarchaeota. *Trends Microbiol.* 18, 331–340. doi: 10.1016/j.tim.2010.06.003
- Stern, R. J., Kohut, E., Bloomer, S. H., Leybourne, M., Fouch, M., and Vervoort, J. (2006). Subduction factory processes beneath the Guguan cross-chain, Mariana Arc: no role for sediments, are serpentinites important?. *Contrib. Mineral. Petrol.* 151, 202–221. doi: 10.1007/s00410-005-0055-2
- Ta, K., Peng, X., Xu, H., Du, M., Chen, S., Li, J., et al. (2019). Distributions and Sources of Glycerol Dialkyl Glycerol Tetraethers in Sediment Cores From the Mariana Subduction Zone. *J. Geophys. Res. Biogeosci.* 124, 857–869. doi: 10.1029/2018JG004748
- Tao, S., Wang, C., Du, J., Liu, L., and Chen, Z. (2015). Geochemical application of tricyclic and tetracyclic terpanes biomarkers in crude oils of NW China. *Mar. Pet. Geol.* 67, 460–467. doi: 10.1016/j.marpetgeo.2015.05.030
- Tarn, J., Peoples, L. M., Hardy, K., Cameron, J., and Bartlett, D. H. (2016). Identification of Free-Living and Particle-Associated Microbial Communities Present in Hadal Regions of the Mariana Trench. *Front. Microbiol.* 7:665. doi: 10.3389/fmicb.2016.00665
- Weber, Y., Sinninghe Damsté, J. S., Zopfi, J., De Jonge, C., Gilli, A., Schubert, C. J., et al. (2018). Redox-dependent niche differentiation provides evidence for multiple bacterial sources of glycerol tetraether lipids in lakes. *Proc. Natl. Acad. Sci. U. S. A.* 115, 10926–10931. doi: 10.1073/pnas.1805186115
- Weijers, J. W. H., Schefuß, E., Kim, J.-H., Sinninghe Damsté, J. S., and Schouten, S. (2014). Constraints on the sources of branched tetraether membrane lipids in distal marine sediments. *Org. Geochem.* 72, 14–22. doi: 10.1016/j.orggeochem.2014.04.011
- Weijers, J. W. H., Schouten, S., van den Donker, J. C., Hopmans, E. C., and Sinninghe Damsté, J. S. (2007). Environmental controls on bacterial tetraether membrane lipid distribution in soils. *Geochim. Cosmochim. Acta* 71, 703–713. doi: 10.1016/j.gca.2006.10.003
- Wenger, L. M., and Isaksen, G. H. (2002). Control of hydrocarbon seepage intensity on level of biodegradation in sea bottom sediments. *Org. Geochem.* 33, 1277–1292. doi: 10.1016/S0146-6380(02)00116-X
- Wu, X. (2014). *The Application Of Glycerol Dialkyl Glycerol Tetraether In Reconstruction Of Kusai Lake Paleo-Environment On The Qinghai-Tibetan Plateau. (in chinese)*. Ph.D. thesis, Beijing: University of Chinese Geosciences.
- Xiao, W., Wang, Y., Liu, Y., Zhang, X., Shi, L., and Xu, Y. (2019). Predominance of hexamethylated 6-methyl branched glycerol dialkyl glycerol tetraethers in the Mariana Trench: source and environmental implication. *Biogeosciences* 17, 2135–2148. doi: 10.5194/bg-17-2135-2020
- Xiao, W., Wang, Y., Zhou, S., Hu, L., Yang, H., and Xu, Y. (2016). Ubiquitous production of branched glycerol dialkyl glycerol tetraethers (brGDGTs) in global marine environments: a new source indicator for brGDGTs. *Biogeosciences* 13, 5883–5894. doi: 10.5194/bg-13-5883-2016
- Xu, Y., Jia, Z., Xiao, W., Fang, J., Wang, Y., Luo, M., et al. (2020). Glycerol dialkyl glycerol tetraethers in surface sediments from three Pacific trenches: distribution, source and environmental implications. *Org. Geochem.* 147:104079. doi: 10.1016/j.orggeochem.2020.104079
- Yamamoto, M., Shimamoto, A., Fukuhara, T., and Tanaka, Y. (2016). Source, settling and degradation of branched glycerol dialkyl glycerol tetraethers in the

marine water column. *Geochim. Cosmochim. Acta* 191, 239–254. doi: 10.1016/j.gca.2016.07.014

Zhang, Z.-X., Li, J., Chen, Z., Sun, Z., Yang, H., Fu, M., et al. (2020). The effect of methane seeps on the bacterial tetraether lipid distributions at the Okinawa Trough. *Mar. Chem.* 225:103845. doi: 10.1016/j.marchem.2020.103845

Conflict of Interest: The authors declare that the research was conducted in the absence of any commercial or financial relationships that could be construed as a potential conflict of interest.

The handling editor declared a past collaboration with several of the authors JL and HX.

Copyright © 2021 Li, Chen, Li, Chen, Xu, Ta, Dasgupta, Bai, Du, Liu and Peng. This is an open-access article distributed under the terms of the Creative Commons Attribution License (CC BY). The use, distribution or reproduction in other forums is permitted, provided the original author(s) and the copyright owner(s) are credited and that the original publication in this journal is cited, in accordance with accepted academic practice. No use, distribution or reproduction is permitted which does not comply with these terms.